



Published in final edited form as:

Biochemistry. 2017 July 05; 56(26): 3337–3346. doi:10.1021/acs.biochem.7b00286.

Biosynthesis of single thioether c-type cytochromes provide insight into mechanisms intrinsic to holocytochrome c synthase (HCCS)

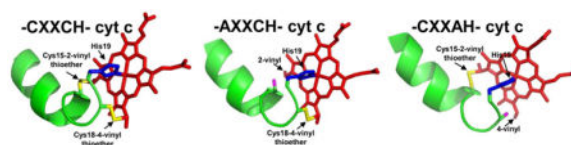
Shalon E. Babbitt, Jennifer Hsu, Deanna L. Mendez, and Robert G. Kranz*

Department of Biology, Washington University, St. Louis, Missouri 63130

Abstract

c-type cytochromes (cyts c) are generally characterized by the presence of two thioether attachments between heme and two cysteine residues within a highly conserved CXXCH motif. Most eukaryotes use the System III cyt c biogenesis pathway comprised of holocytochrome c synthase (HCCS) to catalyze thioether formation. Some protozoan organisms express a functionally equivalent, natural variant of cyt c with an XXXCH heme-attachment motif, resulting in a single covalent attachment. Previous studies have shown that recombinant HCCS can produce low levels of the XXXCH single thioether variant. However, cyt c variants containing substitutions at the C-terminal cysteine of the heme-attachment site (*i.e.* resulting in CXXXH) have never been observed in nature and attempts to biosynthesize a recombinant version of this cyt c variant have been largely unsuccessful. In this study, we report the biochemical analyses of an HCCS-matured CXXXH cyt c variant, comparing its biosynthesis and properties to the XXXCH variant. Results indicate that although HCCS mediates heme attachment to the N-terminal cysteine in CXXXH cyt c variants, up to 50% of the cyt c produced is modified in an oxygen-dependent manner, resulting in a mixed population of cyt c. Since this aerobic modification only occurs in the context of CXXXH, we also propose that natural HCCS-mediated heme attachment to CXXCH likely initiates at the C-terminal cysteine.

Graphical abstract



INTRODUCTION

Cytochrome c (cyt c) plays a vital role in prokaryotes and eukaryotes as an essential component of respiration, for example serving as an electron shuttle in mitochondria between complexes III (cytochrome bc₁) and IV (cytochrome aa₃ oxidase).^{1, 2} A heme cofactor is covalently attached to cyt c via thioether linkages between two vinyl groups of

*To whom correspondence should be addressed: Robert G. Kranz, Department of Biology, Washington University, 1 Brookings Drive, Campus Box 1137, St. Louis, MO, USA, Tel: (314) 935-4278; kranz@biology.wustl.edu.

heme and two cysteines in a conserved Cys-Xxx-Xxx-Cys-His (CXXCH) motif. The histidine of CXXCH serves as an axial ligand to the heme iron. Prokaryotes use one of two multi-component pathways to accomplish the covalent attachment of heme to c-type cytochromes (*i.e.* System I or System II)³⁻⁵, while most eukaryotes use holo-cytochrome c synthase, HCCS (System III), in the mitochondrial intermembrane space.⁶⁻⁹

Although HCCS has long been recognized as the key enzyme in mitochondrial cyt c assembly⁶, investigation of its mechanism, including substrate binding, have only recently been explored (Figure 1A)¹⁰⁻¹³. HCCS-mediated cyt c biosynthesis is proposed to follow a four-step process: In step 1, HCCS binds noncovalently to heme (Fe²⁺), with His154 forming an axial ligand to the heme iron (residue numbering refers to human HCCS).^{10, 11} In step 2, holo-HCCS (*i.e.* heme-bound HCCS) binds to apocyt c, with His19 of CXXCH occupying the second axial ligand position on the heme iron (numbering refers to human cyt c, including its initiating methionine (Figure 1C))¹²; His19 ligation positions Cys18 next to the heme-4 vinyl, while the N-terminal alpha helix-1 of cyt c positions Cys15 next to the heme-2 vinyl.¹³ In step 3, the cysteine thiols spontaneously form stereospecific thioether bonds with the heme vinyls (*i.e.* the thiol groups (-SH) of Cys15 and Cys18 form covalent bonds with the heme 2- and 4-vinyl groups, respectively) (Figure 1A)¹². In step 4, holo-cyt c (*i.e.* heme-attached to cyt c) is released from HCCS to undergo folding. It is proposed that the release process is facilitated by the His19 ligand of cyt c, and by the distortion of heme resulting from both thioether attachments¹².

Widespread conservation of the CXXCH motif in cyt c *a priori* suggests that covalent attachment of heme to the two cysteine residues is central to its optimal stability and activity. However, mitochondrial c-type cytochromes (*i.e.* cyt c and cyt c₁) from a unique class of eukaryotes within the phylum Euglenozoa (*e.g.* *Crithidia fasciculata*, *Trypanosoma brucei*, and *Euglena gracilis*) contain an uncharacteristic XXXCH heme-attachment motif (Figure 1C), resulting in only a single thioether between heme and the second cysteine residue.¹⁴⁻¹⁶ The structural and functional properties of this natural single thioether variant are very similar to that of horse heart cyt c, indicating that a single thioether linkage to the first cysteine (*i.e.* CXXXH) is physically feasible.^{14, 17-20}

Single thioether cyt c variants (with XXXCH) have also been biosynthesized using recombinant or native HCCS.^{10, 12, 20-23} Our initial studies with human single cysteine cyt c variants and recombinant human HCCS analyzed C15S and C18A substitutions, showing that complexes between these cyt c variants and HCCS form, thus both variants are recognized by HCCS and both are competent for heme attachment. It was determined that C15S is released from HCCS at higher levels (10% WT cyt c levels) than C18A (<3% WT cyt c levels).¹⁰ It was also shown that heme in the HCCS/C15S cyt c complex is more distorted (nonplanar *i.e.* “puckered”) than in the HCCS/C18A cyt c complex (as determined by resonance Raman (rR) spectroscopy).¹² These results could be due to 1) the differential impacts of serine and alanine on heme distortion (and thus release) or 2) the possibility that the degree of heme distortion induced by a single thioether attachment to Cys15 is inadequate to facilitate product release. The notable absence of CXXXH-containing single thioether cyt c variants in nature may reflect natural selection against substitution because of an innate defect in the variant (*e.g.* stability or redox potential). Alternatively, absence of this

variant could be due to mechanistic problems with HCCS-mediated biosynthesis of such substrates.

In the present study, we engineered alanine and serine substitutions at both the Cys15 and Cys18 positions in cyt *c*, examining their release from HCCS and their properties. We overcome previous challenges that limited the adequate maturation and release of cyt *c* variants lacking a second thioether (*i.e.* CXXXH (C18A/S)) by exploiting the enhanced product-release feature of a previously characterized HCCS mutant (*i.e.* Glu159Ala).¹¹ We very recently have shown that this HCCS “release mutant” biosynthesizes sufficient levels of CXXXH (*i.e.* C18A/S) cyt *c* variants²² for the biochemical analysis described here. Because redox potential and stability of a C18S cyt *c* variant are similar to WT, there does not appear to be selection against this variant. However, substitutions of the second cysteine (*i.e.* Cys18) result in 2 forms of this single thioether cyt *c* when matured by HCCS, one of which is modified in an oxygen-dependent manner. We propose that this oxygen-associated modification precludes the existence of a CXXXH cyt *c* in nature and that thioether attachment occurs first at Cys18 (of “CH”) to the heme 4-vinyl in step 3 (Figure 1A).

EXPERIMENTAL PROCEDURES

Construction of strains and plasmids

Plasmids used in this study, pRGK403 (N-terminal GST-tagged human HCCS), pRGK405 (human cyt *c* (CYCS)), pRGK417 (C15S cyt *c*), pRGK418 (C18A cyt *c*), and HCCS_E159A (N-terminal GST-tagged human HCCS with Ala substitution at Glu159) have been described previously.^{10, 11} All other oligonucleotide primer sequences and derived plasmids are reported in Supplemental Table 1 (Table S1). The addition of a C-terminal hexahistidine (6x-His) tag and nucleotide substitutions were engineered using the QuikChange II Site-Directed Mutagenesis kit (Agilent Technologies) according to the manufacturer’s specifications. All cloning steps were confirmed by sequencing. Verified clones were transformed into the *E. coli ccm* strain RK103.²⁴

Cyt *c* purification

The purification of HCCS-released cytochrome *c* was performed as previously described.¹² Briefly, *ccm E. coli* carrying plasmids for GST-HCCS (WT or E159A mutant) and cyt *c* (WT or variant, with or without a hexahistidine tag) were inoculated into 100 mL LB supplemented with the appropriate antibiotics, grown overnight at 37°C with shaking, and used to inoculate 1 L LB. Following 1 hour growth of the 1 L cultures at 37°C with shaking at 120 rpm, the cultures were induced with 0.1 mM IPTG for expression of HCCS. 2 hours after the induction of HCCS expression, arabinose was added to 0.2% (wt/vol) to induce expression of CYCS overnight. Cells were harvested by centrifugation at 4,500 × g, resuspended in 50 mM Tris (pH 8) with 1 mM PMSF, and sonicated. The crude sonicate was clarified by centrifugation at 24,000 × g for 20 minutes, and the soluble fraction was isolated by ultracentrifugation at 100,000 × g for 45 minutes. The supernatant was loaded onto CM Sepharose Fast Flow resin (GE Healthcare) for an overnight batch pull-down of positively charged proteins (including cyt *c*). Bound proteins were eluted with either 50 mM Tris (pH 8), 500mM NaCl (for untagged cyt *c*) or 50 mM NaH₂PO₄ (pH 7.4), 300 mM NaCl, 10 mM

imidazole (for 6x-His tagged cyt c). His-tagged cyt c eluant was then incubated with Talon Metal Affinity resin (Clontech) for 30 minutes and eluted with 50 mM NaH₂PO₄ (pH 7.4), 300 mM NaCl, 150 mM imidazole. Cyt c proteins (His-tagged or untagged) were then concentrated in a Vivaspin Turbo centrifugal filter (Thermo Scientific) with a 3 kD cutoff, and total protein concentration was determined using the Bradford reagent (Sigma).

Oxygen limitation assay

ccm E. coli carrying plasmids for His-tagged cyt c (WT, C15A/S, and C18A/S) and GST-tagged E159A HCCS were inoculated into 100 mL LB supplemented with appropriate antibiotics, grown overnight at 37°C with shaking, and used to inoculate 1L of LB in either a 2 L Erlenmeyer flask (for normal and High O₂ conditions) or a capped 1 L bottle (for low O₂ conditions) under the following aeration conditions: 1) low O₂: in which air was maximally excluded (with LB medium) from a sealed bottle that was minimally agitated (50 rpm), 2) Normal O₂: in which air occupied half of a loosely covered culture flask that was agitated at a moderate speed (120 rpm), and 3) High O₂: in which air occupied half of a loosely covered culture flask that was agitated at a high speed (200 rpm). Following 1 hour growth of the cultures at 37°C with shaking, the cultures were induced with 0.1 mM IPTG for expression of E159A HCCS, followed by 0.2% (wt/vol) arabinose for expression of cyt c overnight. Cells were harvested, His-tagged cyt c was purified as described above, and samples were prepared for SDS-PAGE.

Heme stains, Sypro Ruby and Coomassie protein staining, and immunoblotting

Heme staining and Sypro Ruby blot staining were performed as described previously.^{12, 25} Briefly, protein samples were prepared for SDS-PAGE with loading dye that did not contain reducing agents and the samples were not boiled. Following electrophoresis, proteins were transferred to nitrocellulose membranes, which was incubated in the Supersignal Femto kit (Thermo Scientific) chemiluminescent reagent. Heme stain signal was developed by either the Odyssey Fc Imaging System (LI-COR Biosciences) or the ImageQuant LAS4000 Mini detection system (Fujifilm-GE Healthcare). Following heme staining, membranes were washed in PBS and treated with fixing solution (7% acetic acid, 10% methanol (vol/vol)). The membranes were washed in deionized water, stained with Sypro Ruby protein blot reagent (Molecular Probes), and washed again in deionized water. Sypro-stained proteins were visualized with the ImageQuant LAS4000 Mini detection system using the Y515-Di filter or with the Odyssey Fc Imaging System. The membranes were then blocked in PBS containing 5% milk protein (wt/vol). Blots were probed with a 1:2000 dilution of antiserum against cyt c (previously described in ref. 13) and then washed with PBS. Protein A peroxidase (Sigma) was used as a secondary label for detection. The chemiluminescent signal for anti-cyt c was developed using the Immobilon Western kit (Millipore) and detected by either the ImageQuant LAS mini detection system or the Odyssey Fc Imaging System. For Coomassie stains, proteins resolved by SDS-PAGE were stained, destained, and imaged as described previously.¹³

Spectroscopy

UV-vis absorption spectra were recorded with a Shimadzu UV-1800 spectrophotometer at room temperature. Pyridine heme spectra were performed as described previously.²⁶

Briefly, 0.5 M NaOH and pyridine were added to 100 μ g purified protein to yield final concentrations of 100 mM NaOH and 20% pyridine (vol/vol). Samples were chemically reduced with the addition of solid sodium dithionite (sodium hydrosulfite) and UV-vis spectra were recorded from 500 to 600 nm.

Circular dichroism (CD) of cyt c was performed as previously described.²² Briefly, purified His-tagged cyt c samples were buffer exchanged into 50 mM phosphate buffer, pH 7.4, 50 mM NaCl. Samples were standardized by heme concentration and recorded on a Jasco J-815 CD spectrophotometer at room temperature at a continuous scanning speed of 50 nm/min for 5 cumulative measurements. The response rates for far-UV and near-UV recordings were 0.5 and 1 second, respectively. Instrument sensitivity was set to 100 mdeg, with a data pitch of 0.5 nm, and bandwidth of 1 nm.

Determination of cyt c reduction potential

Redox potentials of cyt c were determined as previously described.^{27, 28} Briefly, purified cyt c samples in 50 mM phosphate, pH 7.4, 50 mM NaCl were oxidized with $K_3Fe(CN)_6$ and desalted on a Zeba Spin Desalting column (Thermo Fisher Scientific). The redox dye dichlorophenolindophenol (DCPIP) ($E_m = +217$) was added to yield a Soret absorbance equivalent to that of the heme contained in the cyt c sample. The redox reaction was initiated with the addition of xanthine/xanthine oxidase at a 2:1 substrate/enzyme ratio. UV-vis spectra were recorded every 30 seconds on a Shimadzu UV-1800 spectrophotometer until reduction (of cyt c heme and DCPIP) was complete. All steps were performed at room temperature within an anaerobic airlock chamber (COY). The changes in absorption were analyzed by the Nernst equation: $[25 \text{ mV} \ln (\text{heme}_{\text{red}}/\text{heme}_{\text{ox}})]$ for the one-electron reduction of heme and $[12.5 \text{ mV} \ln (\text{dye}_{\text{red}}/\text{dye}_{\text{ox}})]$ for the two-electron reduction of DCPIP. Calculated cyt c heme Nernst equation values were plotted against those values calculated from the DCPIP Nernst equation on the x- and y-axes, respectively, yielding a straight line in which the y-intercept represents the difference in reduction potential between cyt c heme and DCPIP (of known potential).

Intact protein mass spectrometry

Purified His-tagged cyt c variants were analyzed by mass spectrometry as previously described.²² Briefly, cyt c protein samples in 50 mM NaH_2PO_4 , pH 7.4, 300 mM NaCl, 150 mM imidazole were loaded onto a desalting C8 trap column, eluted by a linear HPLC gradient, and injected into a MaXis-4G Q-ToF mass spectrometer for analysis. Protein mass data was imported into MagTran software²⁹ for mass deconvolution.

RESULTS

XXXCH cyt c variants: Cys15Ala and Cys15Ser

In our *E. coli* recombinant system, membrane-bound HCCS¹⁰ releases cyt c into the bacterial cytoplasm, which is purified from the soluble fraction by ion exchange chromatography (Figure 2A).^{12, 22} For higher purity, a polyhistidine tag (6x-His) was added to the C-terminus for a cobalt-affinity chromatography step (Figure 2A). Single thioether cyt c variants were constructed at the Cys15 position (*i.e.* C15A and C15S cyts c, see Figure

1C). The C15A and C15S cyt c variants were both released from HCCS at similar levels, approximately 10% of WT cyt c, sufficient for purification and characterization by SDS-PAGE (Figure 2B). Both variants contain heme and react with cyt c antisera (Figures 2C, D). Using mass spectrometry, heme attachment to WT and both Cys15 cyt c-6xHis variants was apparent in the total mass calculations of the intact protein (Figure 2E–G).

Like untagged cyt c, ferrous WT cyt c-6xHis exhibits a distinctive alpha peak maximum at 549.5 nm in its visible absorption spectrum (derived from the porphyrin $\pi \rightarrow \pi^*$ electronic transition)³⁰ (Figure 3A, top) and pyridine hemochrome spectrum (Figure 3A, bottom), characteristic of cyt c containing two thioethers.^{26, 31} By contrast, the spectral properties of C15A and C15S cyts c-6xHis are indicative of a single thioether at the remaining cysteine in the heme attachment site (*i.e.* Cys18) (Figure 3B, C). The alpha peak maxima of both C15A and C15S cyts c are red-shifted (*i.e.* shifted to higher wavelength) to 556 nm and 559 nm, respectively (Figure 3B, C, top), with both variants exhibiting an asymmetrical shoulder at 552 nm (Figure 3B, C, top). The asymmetry in the α/β region of both Cys15 cyt c variants is very similar to that observed in the visible spectra from the single thioether cyts c purified from Euglenid protozoans.¹⁴ The difference in alpha peak maxima by 3 nm for C15A (556 nm) and C15S (559 nm) cyt c (Figure 3B, C, top) suggests that alanine and serine differentially impact the heme environment, but importantly, this change does not impact the cyt c levels released from HCCS. Reduced pyridine hemochrome alpha maxima values for C15A (552.6 nm) and C15S (551.4 nm) confirm the presence of a single covalent attachment to heme (Figure 3B, C, bottom), values between that expected for two covalent attachments (549–550 nm, as with WT cyt c) and no covalent attachments (555–556 nm, as with b-type heme).^{1, 31, 32}

The reduction potential of the C15S variant was nearly identical to that of WT cyt c (Table 1 and Figure S1), which was also observed for the midpoint potentials of natural Euglenozoan cytochromes when compared to conventional cyt c.¹⁷ This is similar to reports for the yeast Cys14Ser iso-1-cyt c variant.²¹ A far-UV CD spectrum of human C15S-6xHis cyt c indicates that its alpha helical character is comparable to that of WT cyt c-6xHis, with signature bands at 208 nm and 222 nm (Figure 4A, B). By contrast, the near-UV CD spectrum of C15S-6xHis cyt c indicates that the properties of the bound heme are affected by the single thioether attachment (Figure 4C). While the near-UV CD spectrum of WT cyt c-6xHis exhibited the characteristic signature bands of a c-type cytochrome³³, the human C15S variant showed a distinct negative CD band at 423 nm, similar to the single thioether yeast C14S cyt c.²¹ The thermal stability of C15S cyt c is significantly lower than that of WT³² (Table 1). This finding contrasts with reports of Euglenozoan cyt c stability being relatively comparable to that of horse heart cyt c.¹⁷ However, it is likely that the increased stability of the single thioether cyts c from Euglenid protozoa stems from compensatory sequence features not present in the human C15S cyt c variant engineered here. This result and conclusion is similar to that noted for the *E. coli* recombinant yeast Cys14Ser iso-1-cyt c single thioether variant biosynthesized using yeast HCCS.²¹

CXXXH cyt c variants: Cys18Ala and Cys18Ser

As noted previously^{10, 32}, cyt c variants with residue substitutions at Cys18 are poorly biosynthesized. Accordingly, both C18A and C18S cyt c variants co-expressed with WT HCCS yielded very low levels of released, folded cyt c (<3% WT cyt c).²² Intensity of the heme stain signal from the Cys18 cyt c variants produced by WT HCCS effectively reflect the substantial disparity in protein yields obtained during purification when compared to WT cyt c yields (Figure 5A, compare lanes 3 and 5 with lane 1). This result indicates that both alanine and serine substitutions exhibit similar low levels of release from HCCS (step 4).

To obtain adequate levels of released Cys18 cyt c variants to study, we recently developed the use of selected HCCS “release mutants.”²² One of these HCCS release mutants has an alanine substitution at the conserved Glu159 residue of HCCS, (which is changed to a lysine in the genetic disorder microphthalmia with linear skin defects (MLS)³⁴). The E159A HCCS release mutant facilitates the higher synthesis of cyt c variants with substitutions at axial ligand His19 and at Cys18.²² In that report, it was concluded that these HCCS substitutions affect heme dynamics in the HCCS four step pathway. For C18A and C18S cyt c variants co-expressed with E159A HCCS, we observed a 3 to 9-fold increase in the yields purified from the soluble fraction (Figure 5A, B, compare lanes 4 and 6 with 3 and 5, respectively).

With sufficient protein to analyze, we evaluated the spectral properties of the heme environments within the Cys18 cyt c variants. Interestingly, the α/β absorption region of ferrous C18A and C18S cyt c did not exhibit the asymmetry found in the corresponding peaks of the Cys15 cyt c variants (compare Figure 5C, D, top with Figure 3B, C, top). The absorption maximum values (550 nm) obtained in the reduced pyridine hemochrome spectra for C18A and C18S cyts c closely resemble those measured for WT cyt c (compare Figure 5C, D, bottom with Figure 3A, bottom), which is atypical for single thioether cytochromes (see below). CD measurements showed that while secondary structure of C18S cyt c was like that of WT (Figure 4A, B), electronic properties of the heme environment were similar to the C15S cyt c variant, displaying a negative CD band at 421.5 nm (Figure 4C). The reduction potential of C18S cyt c was within 11 mV of those measured for both WT and the C15S cyt c variant (Table 1 and Figure S1), suggesting that the electron-transfer properties of cyt c are not largely impacted by the loss of the second thioether. C18S cyt c is more stable than C15S cyt c, but less than WT cyt c (Table 1). We propose that redox potential and protein stability are not the reason this single thioether cyt c variant is missing in nature.

By SDS-PAGE, both Cys18 cyt c variants (C18A and C18S) appear to be comprised of two polypeptide species, one electrophoresing the same as WT (and the C15A/S variants) and one at a higher molecular weight. Both species heme stain (Figure 5A) and are recognized by the cyt c antisera (Figures 5B). This “doublet” of cyt c was present whether biosynthesized by WT or E159A HCCS (Figure 5A, B). We presumed that this high molecular weight species represents a modified form of cyt c (referred to as C18A/S-cyt c*) with characteristics possibly contributing to the spectral profiles (Figure 5C, D). To improve sample purity for subsequent mass determination and protein identification, we added C-terminal polyhistidine tags to both Cys18 cyt c variants, and observed that C18A/S-cyt c* continued to co-purify with C18A and C18S cyts c following tandem affinity purification (Figure S2). Intact protein mass spectrometry of purified C18A cyt c-6xHis revealed the

presence of 2 major species (Figure 5E and Table 1). The mass of one was consistent with that expected for the His-tagged, heme-attached cyt c variant (13022.66 Da), while the other differed by an added mass of 16.98 Da (*i.e.* 13039.64 Da). Likewise, the intact masses detected for C18S cyt c-6xHis included a peak corresponding to 13039.65 Da, the expected mass of the variant with heme attached, and another at 13056.67 Da, a value with an additional 17.02 Da (Figure 5F and Table 1). The addition of approximately 17 Da to each Cys18 cyt c variant suggests that a significant fraction of C18A and C18S cyt c is modified with an oxygen and a hydrogen atom, which presumably also alters the electrophoretic mobility of the C18A/S-cyt c* variant by SDS-PAGE (see below and Discussion).

Oxygen limitation reduces modification of CXXXH cyt c (C18A and C18S) variants

We conclude that in HCCS-mediated biosynthesis of Cys18 cyts c (CXXXH), but not Cys15 cyts c variants (XXXCH), an oxygen and a hydrogen atom are added to the product. This occurs whether WT HCCS or the HCCS “release mutant” (E159A HCCS) is used. In our recombinant system, HCCS and cyt c are co-expressed in *E. coli* under normal aeration conditions (*i.e.* conditions that support ample bacterial growth in an aerobic environment). Therefore, oxygen in the culture medium is possibly responsible for this adduct to the Cys18 cyt c variants. We tested whether induction of our recombinant system in *E. coli* grown in different oxygen environments would alter the presence of C18A/S-cyt c* that co-purifies with the C18A and C18S cyt c variants. We co-expressed cyt c-6xHis (WT, C15A/S, and C18A/S) with E159A HCCS in *E. coli* under three aeration conditions, from low oxygen to high oxygen (as described in the Experimental Procedures section). Using heme staining and cyt c immunoblotting, purified WT, C15A, and C15S cyt c-6xHis migrate as single polypeptides at the expected size (~13 kDa with heme attached) on SDS-PAGE in all three conditions (Figure 6A, B, lanes 1-9). However, only the lower O₂ conditions yielded a single protein of expected size for the Cys18 cyt c-6xHis variants (Figure 6A, B, lanes 10, 13, and 14). C18A/S-cyt c* continued to co-purify with the C18A and C18S cyt c-6xHis variants from the moderate and high O₂ conditions (Figure 6A, B, lanes 11-12 and 15). These data are consistent with the proposal that cyt c* contains an oxygen adduct that is added during the HCCS-mediated maturation and/or folding of Cys18 cyt c (see Discussion).

DISCUSSION

Serine vs. Alanine: Impact of residue substitution at Cys15 and Cys18

We previously determined by rR that thioether formation produces significant heme distortion or “puckering” in the HCCS:heme:cyt c ternary complex.¹² We hypothesized that this puckering is sufficient to effect the release of cyt c from the HCCS active site. Having both thioethers, WT cyt c (containing a CXXCH motif) exhibits maximal puckering, and is thus optimally released, while the poorly released, single thioether cyts c, C15S and C18A, contain progressively less heme puckering, respectively. The increased heme distortion (and product release from HCCS relative to that of C18A cyt c) found in C15S cyt c could potentially be due to the serine hydroxyl group. For example, polar properties of the hydroxyl could repel the hydrophobic porphyrin ring, thus generating enough puckering to promote limited release of the C15S cyt c variant. Here we show that exchanging serine for alanine at Cys18 did not result in higher release of the matured human cyt c variant.

Similarly, an alanine at Cys15 did not change its overall yield, which continued to be released at 10% of WT cyt c levels.

In the final released and folded cyt c products, the alanine substitution at Cys15 exhibited slightly different spectral properties than the serine substitution, for example in the alpha absorption peaks of the ferrous forms (Figure 3B, C). Perhaps this is due to the proximity of the serine or alanine side chain to the free 2-vinyl group. In any event, we conclude that serine and alanine substitutions at Cys15 impart similar consequences in the 4-step HCCS mechanism.

E159A HCCS vs. WT HCCS: Properties and release of C18A/S cyt c

Until now, the biosynthesis and characterization of a single thioether cyt c variant with a CXXXH heme-attachment motif had never been described. The challenge in isolating this unnatural cyt c variant stems from its inefficient release by HCCS. We have recently proposed that there exists a delicate balance in the interaction dynamics of heme with HCCS and cyt c that ultimately controls the “trapping” (in the case of the single thioether cyts c) or release of the holocyt c product.¹¹ Using the E159A HCCS “release mutant” to produce the C18A/S cyt c variants effectively shifted this balance towards product release, thus facilitating biosynthesis and purification of C18A/S cyt c for analysis.²²

The UV-vis spectra of ferrous C18A and C18S cyts c are very similar to each other with alpha peaks (~552 nm) that are red-shifted from WT cyt c (~549 nm). This is expected for a single thioether cyt c. The reduced pyridine hemochrome is only approximately 1 nm red-shifted (550 nm for C18A/S cyt c vs. 549 nm for WT cyt c), which is also indicative of one thioether, but may reflect mixed species, one with an oxygen adduct (see below).

To address whether a C18S cyt c variant might be capable of function, we analyzed its thermal stability and redox potential, compared against that obtained for WT and C15S cyt c (Table 1). The reduction potentials of both variants are within 10 mV of the value measured for WT, and C18S is even more thermostable than C15S. We agree with Rosell and Mauk that in the case of Euglenozoan single thioether C15A cyts c, stabilizing, compensatory mutations likely evolved over time.²¹ For substitutions at Cys18, it is just as likely that compensatory mutations could also occur to stabilize this variant.

We conclude that there is no innate property of the CXXXH cyt c variant that would prevent it from occurring in nature. The fact that HCCS “release mutants” can produce C18A/S cyts c also would suggest that recognition and catalysis would not be an impediment to natural biosynthesis. However, we have shown that in the normal, HCCS-mediated aerobic biosynthesis of CXXXH cyt c variants, an anomalous oxygen-dependent modification occurs to the cyt c product. We discuss below how this observation addresses mechanisms behind HCCS function and how it could preclude the evolution of a CXXXH motif in c-type cytochromes.

Cys15 vs. Cys18: Oxygen addition, order of thioether formation, and stereochemistry in HCCS mechanisms

Initial SDS-PAGE of the C18A/S cyt c variants revealed the presence of a slightly higher molecular weight cyt c subspecies (Figure 5A, B, cyt c*). MS analysis determined that these variants were composed of a mixed population of cyt c with expected mass (accounting for the Cys18 substitution and attachment of heme) and cyt c with an additional 17 Da, corresponding to the presence of an oxygen and hydrogen atom. Notably, this additional mass was only present in the C18A/S cyt c variants, suggesting that the elimination of the Cys18 thioether renders cyt c susceptible to modification, likely at the Cys15 single thioether. We propose that the aberrant SDS-PAGE migration of cyt c* could be due to the oxygen adduct.

Cysteine oxidation, in the context of non-canonical heme-attachment motifs, has been observed in previous studies and confirmed through MS analysis.^{35, 36} Although we attempted to confirm the presence and identify the site of the oxygen modification through mass spectrometry of tryptic peptides from independently isolated C18A/S-cyt c*, heme-containing peptides could not be detected, which is often the case for peptides with covalently attached heme.^{37, 38} However, we verified that the presence of oxygen was indeed required for the production of C18A/S-cyt c*, since upon its removal during growth, cyt c* disappeared (Figure 6). Obviously, mitochondria must operate in the presence of oxygen, therefore this adduct addition is likely to affect substrates containing a CXXXH heme attachment motif.

The current study provides a biochemical basis for a preferred order of thioether formation at the CXXCH motif. We propose Cys18 rapidly forms the first thioether at heme 4-vinyl, brought into position by His19 liganding to the heme iron (Figures 1A and S3A). Cys15 then forms the second thioether at heme 2-vinyl, facilitated by the N-terminal alpha helix-1 of cyt c (Figures 1A and S3A). Absence of the CXXXH cyt c motif in nature underscores the importance of the Cys18 thioether, which is the only linkage in Euglenozoan cyt c. We also hypothesize that the observed oxygen-dependent modification of CXXXH cyt c could occur in one of at least two different schemes as a mechanistic consequence of HCCS function during thioether formation: 1) Oxygen could be added to an aberrant thioether linkage formed between the Cys15 thiol and the β carbon of heme 2-vinyl^{35, 39}, or 2) The orientation of heme bound to HCCS could be inverted in up to 50% of the holo-HCCS molecules (Figure 1B), resulting in thioether formation between Cys15 and the heme 4-vinyl, creating an atypical linkage susceptible to oxygen addition. The proposed events are not mutually exclusive, however we present three putative oxygen-modified cyt c: heme products (based on previously described mechanistic schemes)^{35, 39, 40} in favor of the latter scenario (Figure S3B). We note that the maximum amount of C18A/S cyt c* to C18A/S cyt c is 1:1 (*e.g.* see Figure 5A, B). This is consistent with an equal mixture of heme stereoisomers in HCCS.^{41, 42} The near UV CD spectrum for the C18S cyt c variant exhibits negative ellipticity in the Soret region (between 400-450 nm), which is a feature of single covalent linkages²¹ and noncovalent heme.⁴³ However, this feature is also observed in hemoglobin when heme is bound in the inverted orientation.⁴⁴

Thioether bonds in WT cyt c are stereospecific. Although HCCS theoretically can bind both orientations of heme, as we have discussed previously⁹, covalent attachment to WT apocyt c will only occur if heme (Fe²⁺) is bound to HCCS in the proper orientation. It is possible that cyt c His19 drives this stereospecificity as it ligands the heme iron, allowing HCCS to mediate the formation of the first thioether at the adjoining Cys18 to the neighboring heme-4 vinyl (see Figure 1A). In the absence of Cys18 (*i.e.* CXXXH), it is possible that heme attachment stereochemistry is relaxed, thus allowing thioether formation to occur between Cys15 and either heme vinyl group (*i.e.* either orientation, see Figures 1B and S3B). Although the N-terminal alpha helix of cyt c can still position Cys15 at the HCCS active site in the absence of Cys18¹³, it is possible that the correct heme stereochemistry is secured by rapid formation of the Cys18 thioether. The production of C18A/S cyt c* could be due to a slower reaction between the spatially incompatible Cys15 and heme 4-vinyl⁹, while the “normal” C18A/S cyt c variant is properly positioned at the HCCS active site to form the standard, stereospecific attachment between Cys15 and heme 2-vinyl. It is possible that the physical properties of the aberrant linkage of C18A/S cyt c* allow oxygen access to chemically modify the reactive cysteine residue. Although the stereochemical misorientation of heme is speculative at present, the aberrant oxygen-dependent modification in CXXXH cyt c variants presented here demonstrates that such cyt c variants would likely be incompatible with the mitochondrial environment.

Supplementary Material

Refer to Web version on PubMed Central for supplementary material.

Acknowledgments

We thank the Washington University Resource for Biomedical and Bio-organic Mass Spectrometry for protein sample analysis. We also thank Josh Jarodsky for chemical scheme designs. This work was funded by National Institutes of Health Grants R01 GM47909 to RGK and F32 GM108278 to SEB

ABBREVIATIONS

HCCS	holocytochrome c synthase
CD	circular dichroism
WT	wild-type
GST	glutathione-S-transferase
UV-vis	ultraviolet-visible
cyt c	cytochrome c
nm	nanometer
PBS	phosphate buffered saline
IPTG	isopropyl β-D-1-thiogalactopyranoside
6x-His	hexahistidine tag

References

1. Moore, GR., Pettigrew, GW. Cytochromes c. Evolutionary, Structural and Physicochemical Aspects. Springer-Verlag, Heidelberg; Berlin: New York: 1990. p. 115-155.
2. Nicholls, DG., Ferguson, S. Bioenergetics. 4th. Academic Press; 2013.
3. Kranz RG, Richard-Fogal C, Taylor JS, Frawley ER. Cytochrome c biogenesis: mechanisms for covalent modifications and trafficking of heme and for heme-iron redox control. *Microbiol Mol Biol Rev.* 2009; 73:510–528. [PubMed: 19721088]
4. Stevens JM, Mavridou DA, Hamer R, Kritsiligkou P, Goddard AD, Ferguson SJ. Cytochrome c biogenesis System I. *Febs J.* 2011; 278:4170–4178. [PubMed: 21958041]
5. Simon J, Hederstedt L. Composition and function of cytochrome c biogenesis System II. *Febs J.* 2011; 278:4179–4188. [PubMed: 21955752]
6. Dumont ME, Ernst JF, Hampsey DM, Sherman F. Identification and sequence of the gene encoding cytochrome c heme lyase in the yeast *Saccharomyces cerevisiae*. *EMBO J.* 1987; 6:235–241. [PubMed: 3034577]
7. Allen JW. Cytochrome c biogenesis in mitochondria—Systems III and V. *Febs J.* 2011; 278:4198–4216. [PubMed: 21736702]
8. Hamel P, Corvest V, Giege P, Bonnard G. Biochemical requirements for the maturation of mitochondrial c-type cytochromes. *Biochim Biophys Acta.* 2009; 1793:125–138. [PubMed: 18655808]
9. Babbitt SE, Sutherland MC, San Francisco B, Mendez DL, Kranz RG. Mitochondrial cytochrome c biogenesis: no longer an enigma. *Trends Biochem Sci.* 2015; 40:446–455. [PubMed: 26073510]
10. San Francisco B, Bretsnyder EC, Kranz RG. Human mitochondrial holocytochrome c synthase's heme binding, maturation determinants, and complex formation with cytochrome c. *Proc Natl Acad Sci U S A.* 2013; 110:E788–797. [PubMed: 23150584]
11. Babbitt SE, San Francisco B, Bretsnyder EC, Kranz RG. Conserved residues of the human mitochondrial holocytochrome c synthase mediate interactions with heme. *Biochemistry.* 2014; 53:5261–5271. [PubMed: 25054239]
12. Babbitt SE, San Francisco B, Mendez DL, Lukat-Rodgers GS, Rodgers KR, Bretsnyder EC, Kranz RG. Mechanisms of mitochondrial holocytochrome c synthase and the key roles played by cysteines and histidine of the heme attachment site, Cys-XX-Cys-His. *J Biol Chem.* 2014; 289:28795–28807. [PubMed: 25170082]
13. Babbitt SE, Hsu J, Kranz RG. Molecular Basis Behind Inability of Mitochondrial Holocytochrome c Synthase to Mature Bacterial Cytochromes: Defining a critical role for cytochrome c alpha helix-1. *J Biol Chem.* 2016; 291:17523–17534. [PubMed: 27387500]
14. Pettigrew GW, Leaver JL, Meyer TE, Ryle AP. Purification, properties and amino acid sequence of atypical cytochrome c from two protozoa, *Euglena gracilis* and *Crithidia oncopelti*. *Biochem J.* 1975; 147:291–302. [PubMed: 170910]
15. Allen JW, Ginger ML, Ferguson SJ. Maturation of the unusual single-cysteine (XXXCH) mitochondrial c-type cytochromes found in trypanosomatids must occur through a novel biogenesis pathway. *Biochem J.* 2004; 383:537–542. [PubMed: 15500440]
16. Mukai K, Yoshida M, Toyosaki H, Yao Y, Wakabayashi S, Matsubara H. An atypical heme-binding structure of cytochrome c₁ of *Euglena gracilis* mitochondrial complex III. *Eur J Biochem.* 1989; 178:649–656. [PubMed: 2536325]
17. Pettigrew GW, Aviram I, Schejter A. Physicochemical properties of two atypical cytochromes c, *Crithidia* cytochrome c-557 and *Euglena* cytochrome c-558. *Biochem J.* 1975; 149:155–167. [PubMed: 242319]
18. Stellwagen E, Cass R. Alkaline isomerization of ferricytochrome C from *Euglena gracilis*. *Biochem Biophys Res Commun.* 1974; 60:371–375. [PubMed: 4371200]
19. Brems DN, Stellwagen E. Conformational transitions of a cytochrome c having a single thioether bridge. *J Biol Chem.* 1983; 258:10919–10923. [PubMed: 6309822]
20. Fulop V, Sam KA, Ferguson SJ, Ginger ML, Allen JW. Structure of a trypanosomatid mitochondrial cytochrome c with heme attached via only one thioether bond and implications for

- the substrate recognition requirements of heme lyase. *Febs J.* 2009; 276:2822–2832. [PubMed: 19459937]
21. Rosell FI, Mauk AG. Spectroscopic properties of a mitochondrial cytochrome c with a single thioether bond to the heme prosthetic group. *Biochemistry.* 2002; 41:7811–7818. [PubMed: 12056913]
 22. Mendez DL, Babbitt SE, King JD, D’Alessandro J, Watson MB, Blankenship RE, Mirica LM, Kranz RG. Engineered holocytochrome c synthases that biosynthesize new cytochromes c. *Proc Natl Acad Sci U S A.* 2017; 114:2235–2240. [PubMed: 28196881]
 23. Tanaka Y, Kubota I, Amachi T, Yoshizumi H, Matsubara H. Site-directedly mutated human cytochrome c which retains heme c via only one thioether bond. *J Biochem.* 1990; 108:7–8. [PubMed: 2172221]
 24. Feissner RE, Richard-Fogal CL, Frawley ER, Loughman JA, Earley KW, Kranz RG. Recombinant cytochromes c biogenesis systems I and II and analysis of haem delivery pathways in *Escherichia coli*. *Mol Microbiol.* 2006; 60:563–577. [PubMed: 16629661]
 25. Feissner R, Xiang Y, Kranz RG. Chemiluminescent-based methods to detect subpicomole levels of c-type cytochromes. *Anal Biochem.* 2003; 315:90–94. [PubMed: 12672416]
 26. Berry EA, Trumpower BL. Simultaneous determination of hemes a, b, and c from pyridine hemochrome spectra. *Anal Biochem.* 1987; 161:1–15. [PubMed: 3578775]
 27. Efimov I, Papadopoulou ND, McLean KJ, Badyal SK, Macdonald IK, Munro AW, Moody PC, Raven EL. The redox properties of ascorbate peroxidase. *Biochemistry.* 2007; 46:8017–8023. [PubMed: 17580972]
 28. San Francisco B, Bretsnyder EC, Rodgers KR, Kranz RG. Heme ligand identification and redox properties of the cytochrome c synthetase, CcmF. *Biochemistry.* 2011; 50:10974–10985. [PubMed: 22066495]
 29. Zhang Z, Marshall AG. A universal algorithm for fast and automated charge state deconvolution of electrospray mass-to-charge ratio spectra. *J Am Soc Mass Spectrom.* 1998; 9:225–233. [PubMed: 9879360]
 30. Handbook of Metalloproteins. Vol. 1. John Wiley & Sons, LTD; West Sussex, England: 2001.
 31. Daltrop O, Ferguson SJ. Cytochrome c maturation. The in vitro reactions of horse heart apocytochrome c and *Paracoccus denitrificans* apocytochrome c550 with heme. *J Biol Chem.* 2003; 278:4404–4409. [PubMed: 12458205]
 32. Tomlinson EJ, Ferguson SJ. Loss of either of the two heme-binding cysteines from a class I c-type cytochrome has a surprisingly small effect on physicochemical properties. *J Biol Chem.* 2000; 275:32530–32534. [PubMed: 10922364]
 33. Myer YP. Conformation of cytochromes. II. Comparative study of circular dichroism spectra, optical rotatory dispersion, and absorption spectra of horse heart cytochrome c. *J Biol Chem.* 1968; 243:2115–2122. [PubMed: 5648427]
 34. Wimplinger I, Morleo M, Rosenberger G, Iaconis D, Orth U, Meinecke P, Lerer I, Ballabio A, Gal A, Franco B, Kutsche K. Mutations of the mitochondrial holocytochrome c-type synthase in X-linked dominant microphthalmia with linear skin defects syndrome. *Am J Hum Genet.* 2006; 79:878–889. [PubMed: 17033964]
 35. Barker PD, Ferrer JC, Mylrajan M, Loehr TM, Feng R, Konishi Y, Funk WD, MacGillivray RT, Mauk AG. Transmutation of a heme protein. *Proc Natl Acad Sci U S A.* 1993; 90:6542–6546. [PubMed: 8341666]
 36. Ginger ML, Sam KA, Allen JW. Probing why trypanosomes assemble atypical cytochrome c with an AxxCH haem-binding motif instead of CxxCH. *Biochem J.* 2012; 448:253–260. [PubMed: 22928879]
 37. Elias DA, Monroe ME, Marshall MJ, Romine MF, Belieav AS, Fredrickson JK, Anderson GA, Smith RD, Lipton MS. Global detection and characterization of hypothetical proteins in *Shewanella oneidensis* MR-1 using LC-MS based proteomics. *Proteomics.* 2005; 5:3120–3130. [PubMed: 16038018]
 38. Romine MF, Elias DA, Monroe ME, Auberry K, Fang R, Fredrickson JK, Anderson GA, Smith RD, Lipton MS. Validation of *Shewanella oneidensis* MR-1 small proteins by AMT tag-based proteome analysis. *Omics.* 2004; 8:239–254. [PubMed: 15669716]

39. Fee JA, Todaro TR, Luna E, Sanders D, Hunsicker-Wang LM, Patel KM, Bren KL, Gomez-Moran E, Hill MG, Ai J, Loehr TM, Oertling WA, Williams PA, Stout CD, McRee D, Pastuszyn A. Cytochrome rC₅₅₂, formed during expression of the truncated, *Thermus thermophilus* cytochrome c₅₅₂ gene in the cytoplasm of *Escherichia coli*, reacts spontaneously to form protein-bound 2-formyl-4-vinyl (Spirographis) heme. *Biochemistry*. 2004; 43:12162–12176. [PubMed: 15379555]
40. Griesbaum K. Problems and Possibilities of the Free-Radical Addition of Thiols to Unsaturated Compounds. *Angew Chem Int Ed Engl*. 1970; 9:273–287.
41. Guzov VM, Houston HL, Murataliev MB, Walker FA, Feyereisen R. Molecular cloning, overexpression in *Escherichia coli*, structural and functional characterization of house fly cytochrome b5. *J Biol Chem*. 1996; 271:26637–26645. [PubMed: 8900138]
42. LaMar GN, Toi H, Krishnamoorthi R. Proton NMR investigation of the rate and mechanism of heme rotation in sperm whale myoglobin: evidence for intramolecular reorientation about a heme two-fold axis. *J Am Chem Soc*. 1984; 106:6395–6401.
43. Goldberg ME, Schaeffer F, Guillou Y, Djavadi-Ohanian L. Pseudo-native motifs in the noncovalent heme-apocytochrome c complex. Evidence from antibody binding studies by enzyme-linked immunosorbent assay and microcalorimetry. *J Biol Chem*. 1999; 274:16052–16061. [PubMed: 10347156]
44. Santucci R, Mintorovitch J, Constantinidis I, Satterlee JD, Ascoli F. CD studies on the reversed heme orientation in monomeric *Glycera dibranchiata* hemoglobins. *Biochim Biophys Acta*. 1988; 953:201–204. [PubMed: 3349089]

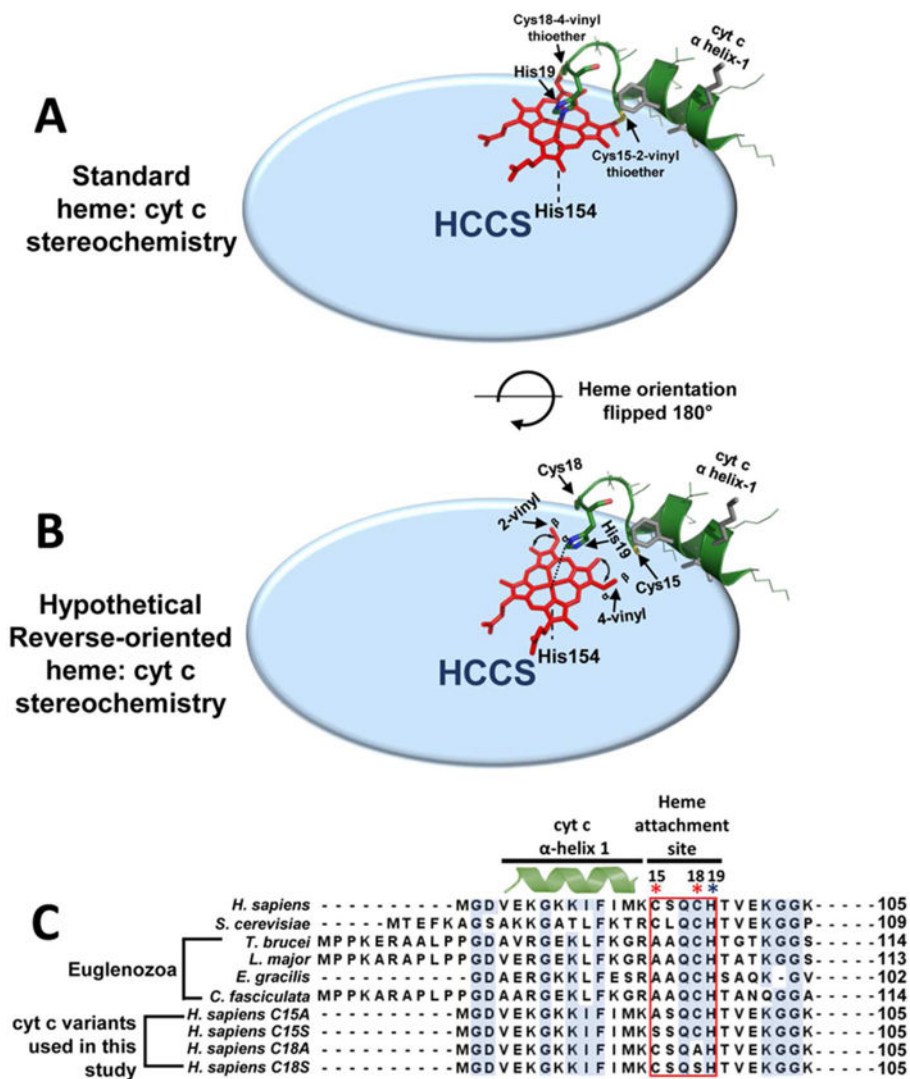


Figure 1. HCCS substrate binding and cyt c sequence alignment

Model of HCCS (blue oval) in complex with its substrates, heme (red) and cyt c (green). A) HCCS-mediated covalent attachment of heme to cyt c with standard stereochemistry. B) HCCS bound to heme in the reverse orientation, which cannot form standard stereospecific thioethers with the cysteine side chains (yellow) in the bound cyt c at the active site. Heme ligands (HCCS His154 and cyt c His19), cyt c: heme thioether attachments (Cys15/2-vinyl and Cys18/4-vinyl), and α - and β -carbons of heme 2- and 4-vinyl are indicated. C) Clustal W-generated amino acid sequence alignment of cyt c N-terminus from human (*Homo sapiens* (UniProt ID P99999)), yeast (*Saccharomyces cerevisiae* (UniProt ID P00044)), and Euglenozoan organisms (*Trypanosoma brucei* (UniProt ID Q57UI4), *Leishmania major* (UniProt ID Q4QEN5), *Euglena gracilis* (UniProt ID P00076), and *Crithidia fasciculata* (UniProt ID P00078)) along with cyt c variants used for this study. Conserved residues are shaded in light blue. Residues within the N-terminal α helix-1 and heme attachment site are indicated. The reactive cysteines and the histidine heme ligand in the CXXCH motif are

denoted with asterisks (*). Residue numbering for the heme attachment site represents that of the human cyt c sequence, with the initiating methionine as position 1.

Author Manuscript

Author Manuscript

Author Manuscript

Author Manuscript

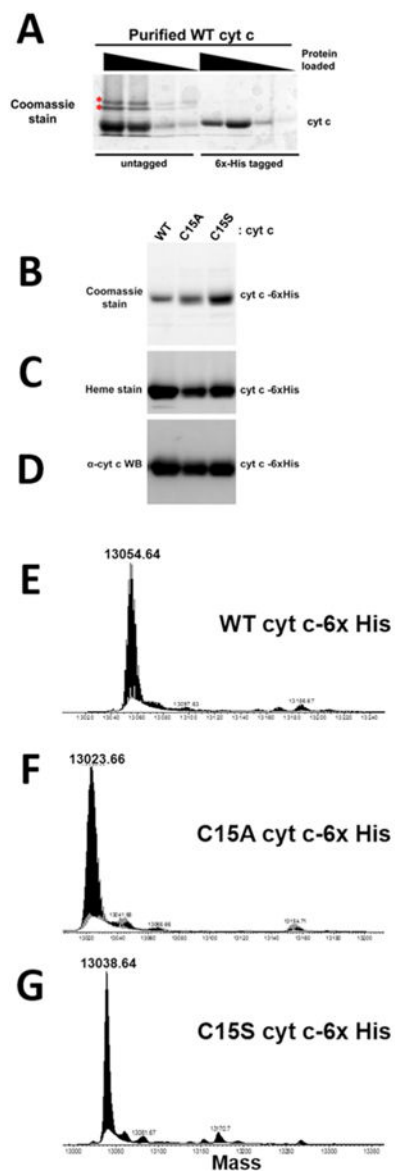


Figure 2. Characterization of HCCS-matured C15A/S cyt c variants

The indicated cyts c were biosynthesized by HCCS, purified from *E. coli*, resolved by SDS-PAGE, and visualized by A-B) Coomassie blue, C) heme stain, and D) immunoblot with cyt c antisera. Red asterisks denote contaminating proteins. In B-D, loaded protein for each sample was standardized to approximately 5 μ g. Mass spectrometry of intact His-tagged E) WT, F) C15A, and G) C15S cyts c are shown with the observed mass in Daltons indicated above each detected peak.

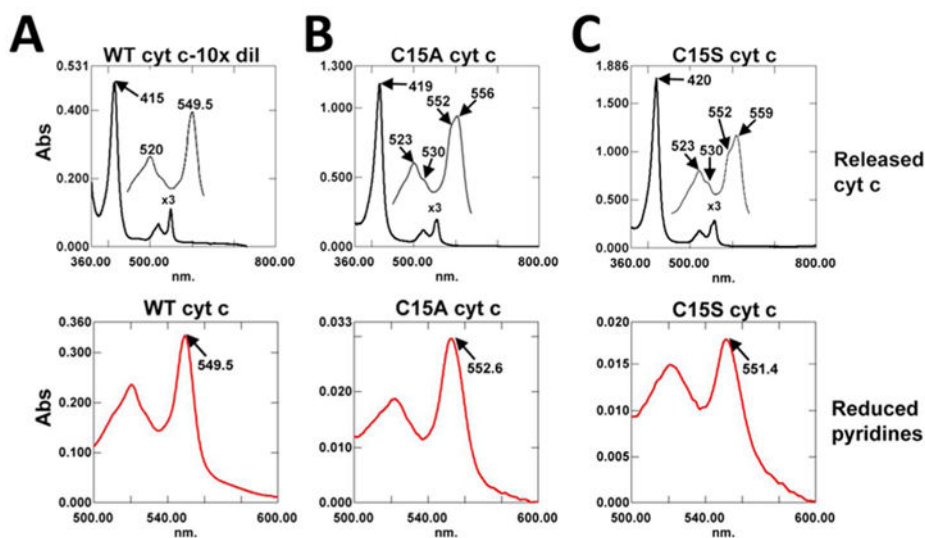


Figure 3. Serine and alanine substitution of Cys15 impact cyt c heme environment
 UV-visible absorption spectra (top) and reduced pyridine hemochrome spectra (bottom) of A) WT, B) C15A, and C) C15S cyts c are shown. All cyt c samples were biosynthesized by HCCS and purified from *E. coli*. For the UV-visible absorption spectra (top) of WT cyt c, 7.6 μ M protein was measured. For all other measurements, 76 μ M protein was used for each sample. Wavelengths (nm) of peak maxima are indicated. A 3-fold enlargement of the α/β absorption bands (between 500 – 600 nm) is shown in the top panels.

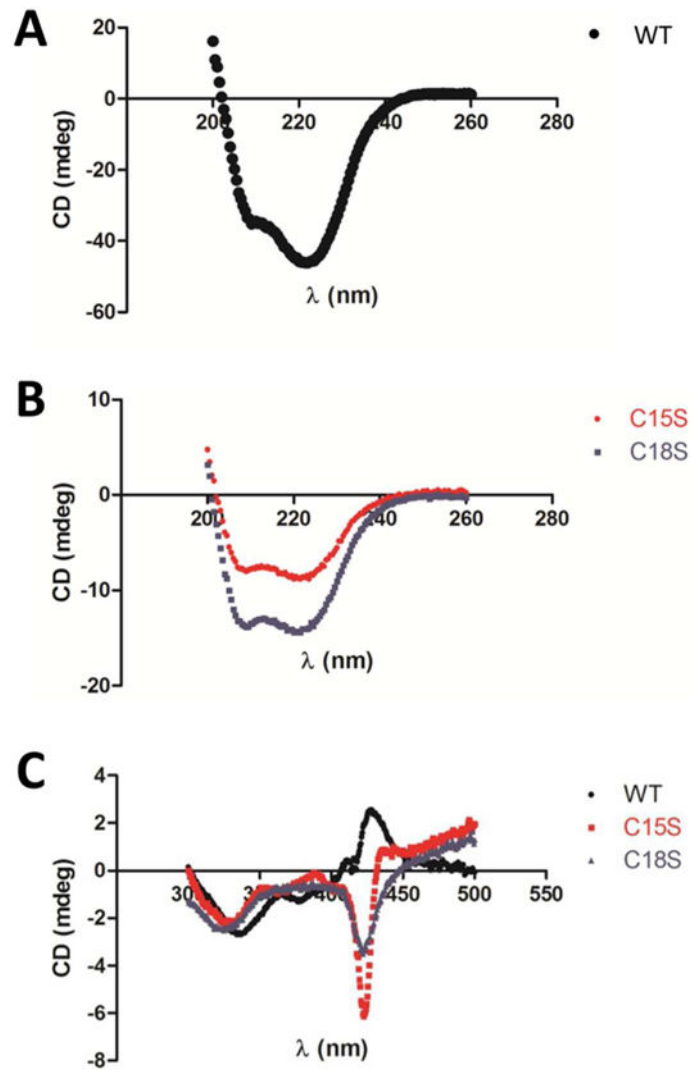


Figure 4. Secondary structure and heme properties of cytochrome c variants
Far UV CD of purified A) WT (black), B) C15S (red) and C18S (blue) cytochromes c. C) Near UV CD of the indicated cytochromes c.

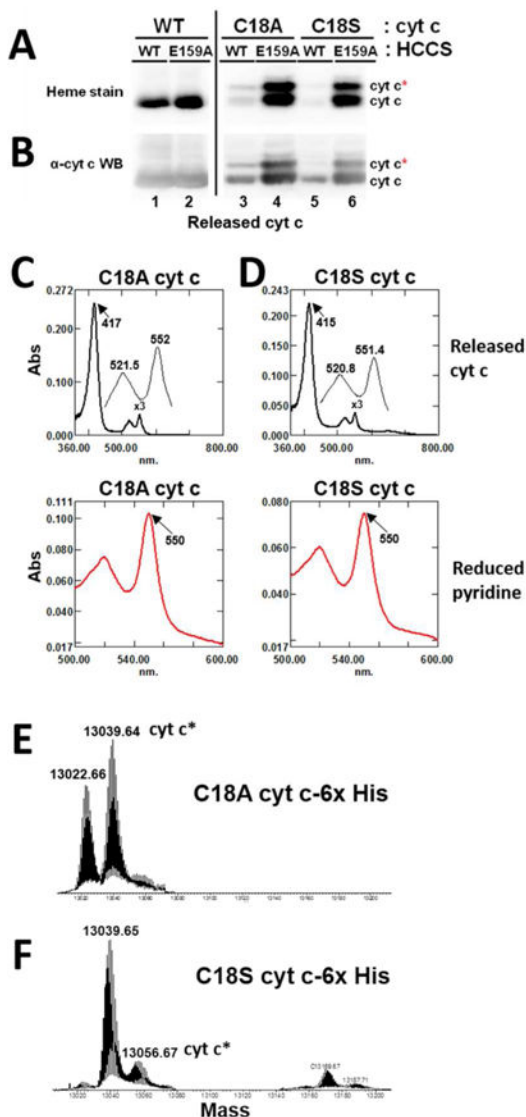


Figure 5. Characterization of HCCS-matured C18A/S cyt c variants

The indicated cyts c were biosynthesized by either WT or E159A HCCS, purified from *E. coli*, resolved by SDS-PAGE, and visualized by A) heme stain and B) immunoblot with cyt c antisera. Protein loading was standardized by volume. UV-visible absorption spectra (top) and reduced pyridine heme spectra (bottom) of C) C18A and D) C18S are shown. Wavelengths (nm) of peak maxima are indicated. 76 μ M protein was measured for each sample. A 3-fold enlargement of the α/β absorption bands (between 500 – 600 nm) is shown in the top panels. Mass spectrometry of intact His-tagged E) C18A and F) C18S cyts c are shown with the observed mass in Daltons indicated above each peak. The oxygen modified cyt c species is denoted as cyt c*.

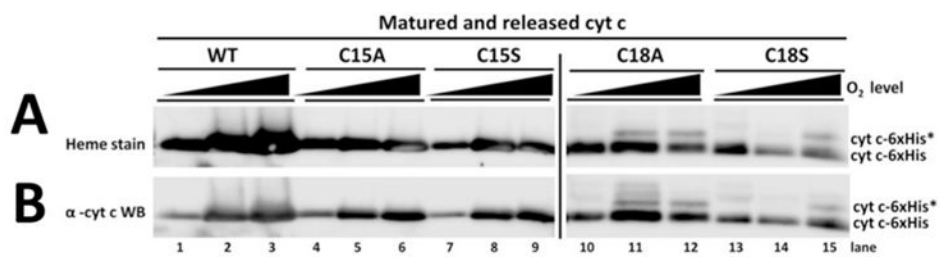


Figure 6. Oxygen-limiting conditions prevent modification of HCCS-matured C18A/S cyt c variants

The indicated cyts c were biosynthesized by E159A HCCS under variable oxygen conditions, purified from *E. coli*, resolved by SDS-PAGE, and visualized by A) heme stain and B) immunoblot with cyt c antisera. Protein loading was standardized by volume

Table 1

Physicochemical characterization of cyt c (WT and single thioether variants)

Cyt c	Mass (Da) ^a		UV-vis spectra peak maxima (ferrous)			Reduced pyridine α maximum (nm)	Redox Potential (E°'/mV)	Denaturation Temp (°C) ^b
	Expected	Observed	Soret (nm)	β (nm)	α (nm)			
WT	13056.79	13054.64	415	520	549.5	549.5	235	85
C15A	13024.69	13023.66	419	523/530	552/556	552.6	nd	nd
C15S	13040.69	13038.64	420	523/530	552/559	551.4	236	50
C18A	13024.69	13022.66	417	521.5	552	550	nd	nd
C18A*	—	13039.64	—	—	—	—	—	—
C18S	13040.69	13039.65	415	520.8	551.4	550	244	70
C18S*	—	13056.67	—	—	—	—	—	—

^aMass of each cyt c was determined by mass spectrometry of intact purified protein. Accuracy of observed masses are within ± 1 Da. Excluding the observed masses reported for C18A* and C18S*, all other detected masses coincided with calculated values expected for each cyt c, which included the full-length polypeptide (initiating Met cleaved), heme, and the C-terminal hexahistidine tag.

^bThermodenaturation temperature curves of each purified cyt c were previously reported.²²